

Multiscale approach to mechanical behavior of polymeric nanocomposites: an application of $T_{1\rho}$ (^{13}C) relaxation experiments at variable spin-locking fields^{*})

Jiří Kotek^{1), **)}, Jiří Brus¹⁾

DOI: dx.doi.org/10.14314/polimery.2014.662

Abstract: The article describes the multiscale experimental approach to the mechanical behavior of polymeric nanocomposites. It is based on a combination of structure sensitive methods with mechanical testing, which allows us to relate macroscopic mechanical behavior on one side, and molecular and supermolecular structure on the other. In addition to widely used X-ray scattering and microscope methods, solid-state NMR is applied in order to obtain information about structure and, primarily, about the dynamics of polymer segments. Particular attention is devoted to $T_{1\rho}$ (^{13}C) relaxation experiments performed at variable ^{13}C spin-locking fields.

Keywords: polyamide 6, nanocomposite, $T_{1\rho}$ (^{13}C) relaxation, molecular dynamics, fracture toughness.

Zależność właściwości mechanicznych nanokompozytów polimerowych od ich struktury określana na podstawie pomiarów czasów relaksacji $T_{1\rho}$ (^{13}C) z zastosowaniem zmiennego pola ujarzmiania spinów

Streszczenie: Opisano sposób oceny właściwości mechanicznych nanokompozytów polimerowych z zastosowaniem połączenia metod wykorzystywanych do określania struktury z technikami służącymi do wyznaczania wytrzymałości mechanicznej materiału. Celem badań było ustalenie relacji między właściwościami mechanicznymi a nadcząsteczkową strukturą polimeru. Strukturę nanokompozytów, a także dynamikę polimerowych segmentów określano też metodami: szerokokątowego rozpraszania promieni X, NMR ciała stałego oraz za pomocą technik mikroskopowych. Szczególną uwagę poświęcono możliwości wykorzystania czasów relaksacji obserwowanych w zmiennym polu ujarzmiania spinów.

Słowa kluczowe: poliamid 6, nanokompozyty, czas relaksacji $T_{1\rho}$ (^{13}C), dynamika molekularna, odporność na kruche pękanie.

Polymeric nanocomposites (NC) derived from layered silicates have received much attention over the last two decades, both in industry and in academia. They exhibit improved stiffness and strength as well as suppressed thermal expansion coefficients and enhanced barrier properties [1]. Moreover, it seems that possible fracture toughness enhancements are system-specific, and thus no systematic predictive methodologies have been developed. A majority of nanocomposite studies have focused on the effects of the silicate surface treatment and concentration on various aspects of these materials. However, knowledge of the deformation and fracture mechanisms of the nanocomposites is rather vague. Only a few studies

have provided comprehensive reports of the fracture behavior of polymeric nanocomposites. Generally, toughness is the only mechanical parameter of polymeric nanocomposites that is not enhanced, but even decreased. In fact, increased toughness was observed only with nanocomposites with inherently brittle matrices like epoxy or polyester resins [2, 3]. It seems that a fully exfoliated nanocomposite does not exhibit efficient toughening mechanisms for length scale and size reasons. Nanoscale reinforcements are by orders of magnitude smaller than the fracture process zone in the crack tip region. Crack tip blunting, which takes place in microcomposites, is not possible with nanoscaled fillers smaller than the radius of gyration of polymer chains. The reduction in ductility and toughness is usually attributed to the constrained mobility of polymer chains in the vicinity of the silicate surface. In these complex materials, however, one cannot expect simple relations between material properties and composition of polymer systems. Large interfacial areas and significantly enhanced surface-to-volume ratios cause unexpected changes in molecular

¹⁾ Academy of Sciences of the Czech Republic, Institute of Macromolecular Chemistry, Heyrovsky Sq. 2, 162 06 Prague 6, Czech Republic.

^{*}) Material contained in this article was presented at the MoDeSt Workshop 2013, Warsaw, Poland, 8–10 September 2013.

^{**)} Author for correspondence; e-mail: kotek@imc.cas.cz

dynamics. Polymer chains spatially close to the nanofiller are confined and this causes the glass-transition temperature T_g to shift to higher temperatures. At the same time, it is supposed that the enhanced chain mobility existing at the surface causes a reduction of T_g in thin polymer films, porous materials and composites with poor interfacial adhesion [4, 5]. Since these effects oppose each other, it is no surprise that both decreases [6–9] and increases [10–12] in T_g in nanocomposites have been reported. It is obvious that the fine relationship between all acting contributions and the final properties of polymer nanocomposites require a deeper investigation of the structure and dynamics of polymer chains.

Our multiscale approach to the mechanical behavior is based on a combination of structure sensitive methods, together with mechanical testing, which allows us to find the relationship between macroscopic mechanical behavior and molecular and supermolecular structure. In addition to widely used X-ray scattering and microscope methods, in order to obtain information about the structure and dynamics of polymer segments. This complex approach is demonstrated on polyamide nanocomposites with layered silicate, as structure-property relationships in polyamide-6/layered silicate nanocomposites have been the subject of our research for a long time [13–16]. In our previous works, we developed domain-selective solid-state NMR experiments [17] for the investigation of the role of motional amplitudes of polymer segments in reducing glass transition temperatures [16]. More recently, we focused our attention on the relationships between fracture toughness and the extent of layered silicate exfoliation [13]. The presence of the layered silicate, its content and the degree of its dispersion were imprinted in a particular way in all mechanical characteristics. While the exfoliated structure imparted higher stiffness and tensile strength to the nanocomposite, its contribution to toughness was not straightforward. Toughness of both the intercalated and exfoliated systems were slightly increased by the addition of 1 wt % of

clay. In the case of exfoliated nanocomposites, toughness then decreased with increasing clay content. For intercalated nanocomposites, the drop in toughness was shifted to higher clay concentrations. At the same time, the toughness was systematically higher in comparison with exfoliated nanocomposites. To understand this difference in mechanical properties at the molecular level, all the prepared nanocomposites were subjected to a detailed investigation by solid-state NMR. It has been shown that toughness is coupled with the amount of the rapidly relaxing component of the amorphous phase [18]. Indeed, the dependences of the intensity of the free domains on the silicate content and dispersion matched well the corresponding trends of fracture toughness, Fig. 1.

In this contribution we report our subsequent investigation attempting to correlate the observed changes in fracture toughness with the dynamics of polymer segments. Particular attention is devoted to $T_{1\rho}(^{13}\text{C})$ relaxation experiments performed at variable ^{13}C spin-locking fields.

EXPERIMENTAL PART

Materials and sample preparation

Two nanocomposite systems derived from a commercial-grade polyamide 6 (PA 6) Ultramid B4 (BASF, Germany) were compared, namely intercalated and fully exfoliated nanocomposites. The silicate dispersion was controlled by different modifications of the silicate surface. This was achieved by melt-compounding of polyamide with sodium montmorillonite and organophilized montmorillonite. This approach made it possible to compare nanocomposites with the same matrix and the same inorganic content but differing in morphology and is described in [13]. While sodium montmorillonite formed intercalated nanocomposites, the organophilization promoted full exfoliation of the silicate layers in the matrix, Table 1.

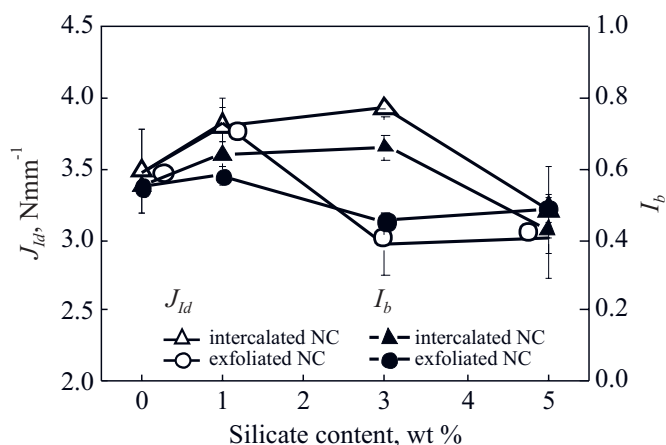


Fig. 1. Toughness, expressed by the critical value of the J -integral, and intensity of rapidly relaxing component, I_b , as a function of the silicate content; data from [13, 18]

Table 1. Composition of studied samples and corresponding glass transition temperatures, T_g

Sample	Silicate content wt %	Layered silicate	T_g , °C
Neat PA 6	–	–	55.0
Intercalated-1	1	Cloisite Na+	48.8
Intercalated-3	3	Cloisite Na+	48.3
Intercalated-5	5	Cloisite Na+	49.0
Exfoliated-1	1	Cloisite 30B	48.0
Exfoliated-3	3	Cloisite 30B	49.2
Exfoliated-5	5	Cloisite 30B	50.0

Methods of testing

Solid-state NMR experiments were measured using a Bruker Avance 500 WB/US NMR spectrometer (Karls-

ruhe, Germany, 2003) at a magic angle spinning (MAS) frequency of 11 kHz. In all cases, the dried samples were placed into ZrO₂ rotors. The domain-selective $T_{1\rho}({}^{13}\text{C})$ relaxation experiments [18, 19] at various intensities of ${}^{13}\text{C}$ spin-locking fields (40, 60 and 80 kHz) were used for measurements of relaxation times separately in mobile and rigid domains (amorphous and crystalline phase, respectively). The experiments were performed at 315 K, and temperature calibration correcting for frictional heating of the samples was performed [20].

Dynamical mechanical thermal analysis was carried out in the torsion mode using an oscillation frequency of 1 Hz, a maximum deformation was allowed of 0.1 %, over a temperature range from 298.15 to 473.15 K (25 to 200 °C), at a heating rate of 3 deg/min. The glass transition temperature, T_g , was defined at the temperature of the maximum value of $\tan(\delta)$.

RESULTS AND DISCUSSION

Segmental motions covering a wide range of time-scales and amplitudes considerably affect the mechanical properties of synthetic polymers. Two distinctive groups of segmental motions are easily recognized via traditional NMR measurements of spin-relaxation times and ${}^1\text{H}$ - ${}^{13}\text{C}$ dipolar couplings: *i*) high-frequency low-amplitude motions (liberations, rotations and jumps of small groups occurring with frequencies about hundreds of MHz); *ii*) and mid-kilohertz frequency (kHz) high-amplitude motions involving the movements of larger parts of polymer chains. The low-frequency motions can be particularly correlated with the thermomechanical material properties such as modulus or glass transition absorbing considerable amounts of mechanical energy.

An insight into the correlation times of low-frequency motions is provided by NMR spin-lattice relaxation measurements in the rotating frame using spin-locking radio-frequency fields. Generally, spin-lattice relaxation is the process of recovery of a spin system into the thermodyna-

mic equilibrium during which the energy of the spin system at a given magnetic field B_0 ($\Delta E = h\gamma B_0/2\pi$) dissipates into the lattice. The recovery of a spin system is induced by fluctuations of local fields and it is most effective when the frequencies of the segmental motions correspond with the Larmor precession frequency, e.g. 125 MHz for ${}^{13}\text{C}$ spins at $B_0 = 11.7$ T. Consequently, measurements of T_1 relaxation times of various nuclei in the laboratory frame (e.g. ${}^1\text{H}$, ${}^{13}\text{C}$ or ${}^{15}\text{N}$) cover a wide range of high-frequency motions (from ca. 500 to 50 MHz at 11.7 T). Analysis of low-frequency motions, however, requires the application of significantly weaker magnetic fields. Experimentally, this is achieved by applying a rotating (spin-locking) B_1 field for which the intensity expressed in frequency units ranges from ca. 10 to 100 kHz. Consequently, measurements of spin relaxation times in the rotating frame ($T_{1\rho}$) open a window into mid-kilohertz motions.

Generally, in polyamide 6 systems, four distinct subpopulations of polymer chains involving two polymorphic crystalline forms α and γ , as well as the “confined” and “free” domains of the amorphous phase, have been identified (Fig. 2a). Consequently, a detailed analysis of the segmental dynamics in these systems required application of domain-selective experiments allowing the selective suppression and/or excitation of different (rigid/mobile) polymer segments. These techniques previously described in the literature [17–19] are based on the measurements of spin-relaxation times specifically selected by $T_1({}^{13}\text{C})$ or inverse- $T_1({}^{13}\text{C})$ relaxation filters for rigid and/or mobile domains of PA6 chains. Moreover, as mentioned above, the $T_{1\rho}({}^{13}\text{C})$ relaxation process is dependent on the intensity of the applied spin-locking $B_1({}^{13}\text{C})$ field. Therefore, we performed three parallel sets of relaxation experiments with variable spin-lock field strength covering a relatively broad range of mid-kilohertz segmental motions (40, 60 and 80 kHz). In this way, we tried to find the most suitable experimental conditions allowing clear distinctions of different high-ampli-

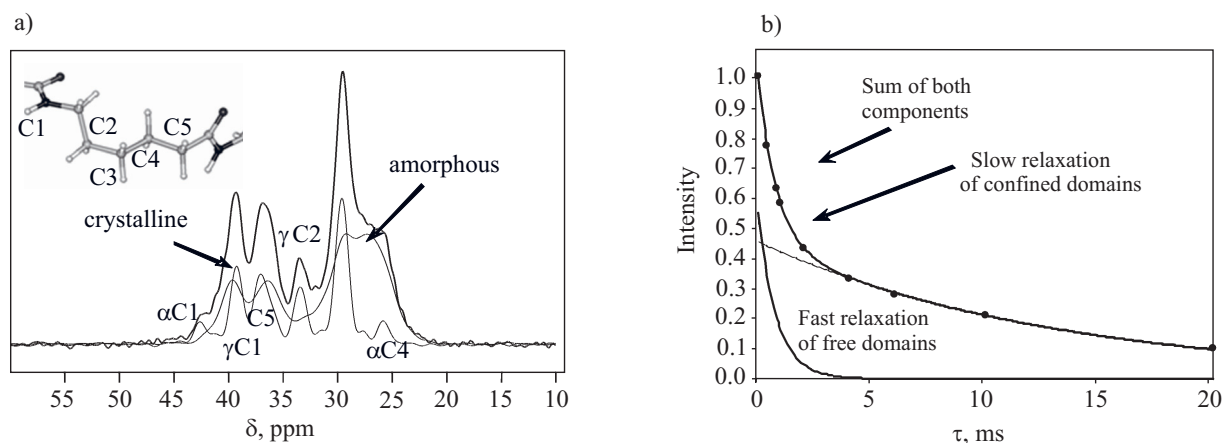


Fig. 2. a) Nonselective and domain-selective ${}^{13}\text{C}$ CP/MAS and ${}^{13}\text{C}$ MAS NMR spectra of intercalated NC and b) $T_{1\rho}({}^{13}\text{C})$ relaxation decay recorded selectively for C1 units in the amorphous domains of intercalated NC

tude mid-kilohertz frequency motional modes involving large polymer segments.

All the recorded $T_{1\rho}(^{13}\text{C})$ relaxation decays clearly exhibited distinct two-component behaviors with the slow and rapid relaxing populations of polymer segments (Fig. 2b). Bearing in mind all the limitations following from the complex mechanism of ^{13}C spin-relaxation in the rotating frame, these two components were attributed to different mid-kilohertz frequency segmental motions. The fast component of $T_{1\rho}(^{13}\text{C})$ falling into the range 0.8–1.2 ms indicates highly efficient spin-relaxation processes that are active during high-amplitude *trans-gauche* jumps that are predominantly present in the “free” domains. In contrast, the slow components of $T_{1\rho}(^{13}\text{C})$ ranging from 10 to 13 ms with high probability reflects relatively low-amplitude wobbling that correspond to less effective motions dominating the “confined” domains of the amorphous phase. Because the small-amplitude motions and high-amplitude *trans-gauche* flips may not be strictly located within the “confined” and “free” domains, respectively, it is reasonable to assume that these motional modes can partially cross-operate. Nevertheless, using a general expression for the double-exponential decay

$$I(\tau) = I_a e^{-\frac{\tau}{T_{1a}}} + I_b e^{-\frac{\tau}{T_{1b}}} \quad (1)$$

a detailed analysis of the obtained relaxation data allowed the extraction of $T_{1\rho}(^{13}\text{C})$ relaxation times (T_{1a} , T_{1b}) and the corresponding intensities (I_a , I_b) for individual CH_2 groups of the PA 6 chains located in the “confined”

and “free” domains. In this way, we found that the relaxation times are basically identical for all the prepared nanocomposites indicating that the internal dynamics of polymer segments within the domains of the amorphous phase, i.e. their motional frequencies, are nearly unaffected by the presence of silicate platelets. On the other hand, the determined intensities of rapidly and slowly relaxing components I_a and I_b exhibit distinct differences indicating changes in the content of “free” and “confined” domains. Although the absolute quantification of the amount of these domains is considerably complicated due to several relaxation processes operating simultaneously, the estimated relative contents of “free” and “confined” domains of the amorphous phase as a function of silicate content basically follow the same trend as fracture toughness (Fig. 1).

These trends are qualitatively comparable for all the relaxation experiments performed at different spin-locking fields (Fig. 3) validating our observations and indicating that the application of a radio-frequency field of 60 kHz allows the most efficient distinction of different motional modes in the amorphous phase of PA 6 systems. In this respect, we found out that the $T_{1\rho}(^{13}\text{C})$ relaxation times determined for the “confined” and “free” domains become slower with increased intensity spin-locking fields. This effect is clearly apparent at 80 kHz when the fast component of $T_{1\rho}(^{13}\text{C})$ ranges from 6 to 8 ms, and the slow component from 12 to 15 ms. As the difference between the fast and slow component of $T_{1\rho}(^{13}\text{C})$ measured at 80 kHz is relatively small, the estimation of the corre-

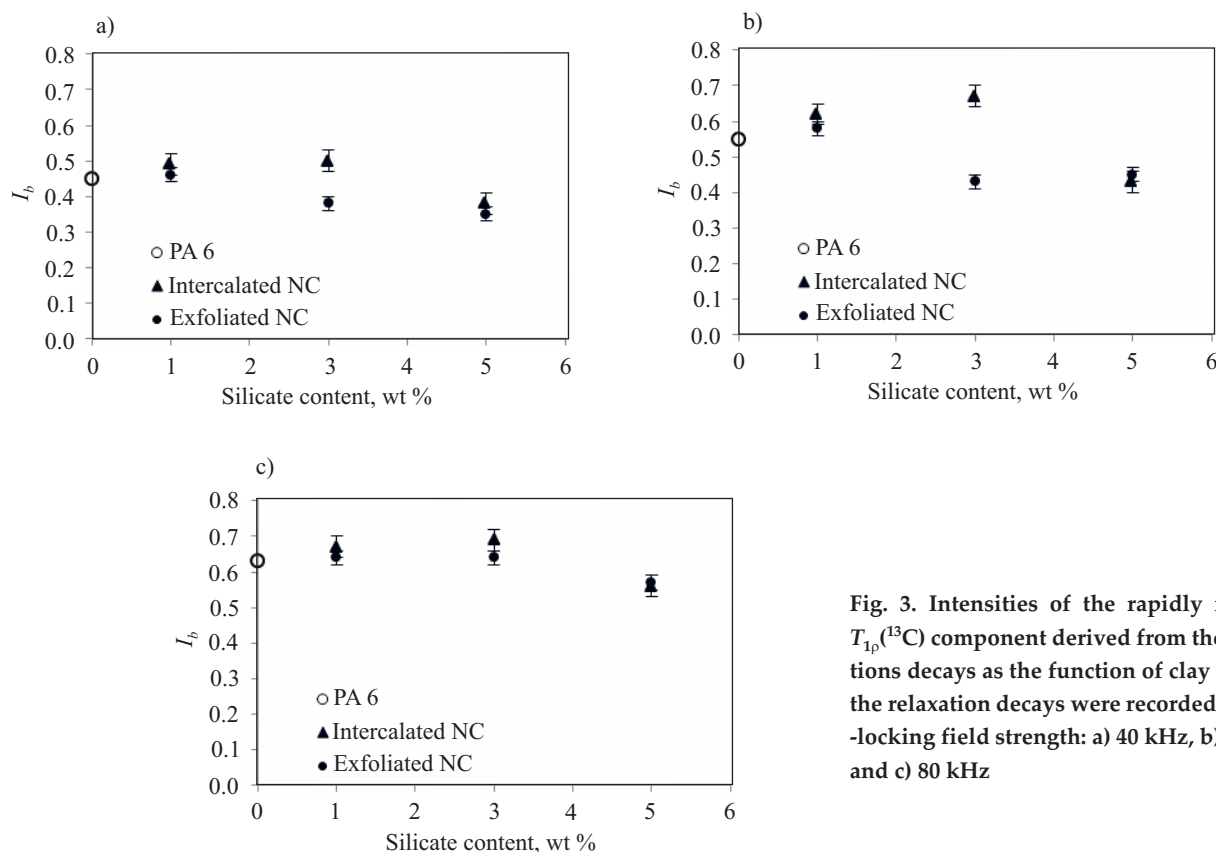


Fig. 3. Intensities of the rapidly relaxing $T_{1\rho}(^{13}\text{C})$ component derived from the relaxation decays as the function of clay content; the relaxation decays were recorded at spin-locking field strength: a) 40 kHz, b) 60 kHz and c) 80 kHz

sponding relative intensities I_a and I_b by the fitting procedure is less reliable. In this particular case the intensity of the "fast" component seems to be overestimated. Overall, considering the experimental error estimated from two independent relaxation measurements performed for each spin-locking field, it is clear that the intensity of the rapidly relaxing component is generally higher in intercalated nanocomposites than in the systems containing smaller amounts of the silicate. On the other hand, the lower instead of this rapidly relaxing component is characteristic for exfoliated systems, especially those containing large amounts of silicate platelets.

The observed changes in molecular dynamics explain not only changes in mechanical behavior as shown in [13, 18] but also changes in the glass transition temperature, T_g . The dynamical mechanical thermal analysis showed clearly that the incorporation of layered silicate into a PA 6 matrix results in a decrease in T_g , Table 1. The T_g markedly drops by almost 7 deg after the addition of 1 wt % of the silicate. The decrease is a little more pronounced for the exfoliated sample. For exfoliated systems, T_g then increases monotonically with increased silicate content. In the case of intercalated nanocomposites, the T_g slightly decreases for the nanocomposite containing 3 wt % of the silicate and then raises increases more for the highest silicate content. The decrease in T_g for PA 6 nanocomposites derived from organically modified layered silicate was reported in [21]. The authors ascribed the observed shift to lower temperatures to the plasticizing effect from the presence of organic modifiers within the silicate. However, this notion can hardly be applied in this case. First, the decrease has been observed for organophilized silicate as well as for a sodium silicate. Second, in exfoliated systems, T_g tends to increase with increased silicate content. It is clear from our data that the explanation is in changes in molecular dynamics.

CONCLUSIONS

It has been demonstrated that the application of domain-selective inverse- T_1 -filtered experiments allows the probing of internal dynamics in complex multicomponent semicrystalline nanocomposites based on PA 6 and layered silicate. Although the small-amplitude motions and high-amplitude *trans-gauche* flips are not strictly located within the "confined" and "free" domains, respectively, applying a set of spin-locking fields we found experimental parameters suitable to estimate the relative amounts of these domains in the amorphous phase of the PA 6 matrix. In this way, we found that certain correlations between spin-dynamics and mechanical properties indicating that segmental mobility of PA 6 chains particularly located in amorphous phase is at least partly related to the thermo-mechanical behavior of these nanocomposites. It has been also shown that toughness is coupled with the amount of the rapidly relaxing component of the

amorphous phase as the dependences of the intensity of the free domains on the silicate content and dispersion matched well with the corresponding trends of fracture toughness.

ACKNOWLEDGMENT

The work was supported by the Czech Science Foundation (project 13-29009S).

REFERENCES

- [1] Ray S.S., Okamoto M.: *Prog. Polym. Sci.* **2003**, 28, 1539. <http://dx.doi.org/10.1016/j.progpolymsci.2003.08.002>
- [2] Zilg C., Mulhaupt R., Finter J.: *J. Macromol. Chem. Phys.* **1999**, 200, 661. [http://dx.doi.org/10.1002/\(SICI\)1521-3935\(19990301\)200:3<661::AID-MACP661>3.0.CO;2-4](http://dx.doi.org/10.1002/(SICI)1521-3935(19990301)200:3<661::AID-MACP661>3.0.CO;2-4)
- [3] Wang K., Chen L., Wu J., Toh M.L., et al.: *Macromolecules* **2005**, 38, 788. <http://dx.doi.org/10.1021/ma048465n>
- [4] Sun Y., Zhang Z., Moon K.S., Wong C.P.: *J. Polym. Sci., Part B* **2004**, 42, 3849. <http://dx.doi.org/10.1002/polb.20251>
- [5] Ash B.J., Schadler L.S., Siegel R.W.: *Mater. Lett.* **2002**, 55, 83. [http://dx.doi.org/10.1016/S0167-577X\(01\)00626-7](http://dx.doi.org/10.1016/S0167-577X(01)00626-7)
- [6] Kalgaonkar R.A., Jog J.P.: *J. Polym. Sci., Part B* **2003**, 41, 3102. <http://dx.doi.org/10.1002/polb.10616>
- [7] Wu Z., Zhou Ch., Qi R., Zhang H.: *J. Appl. Polym. Sci.* **2002**, 83, 2403. <http://dx.doi.org/10.1002/app.10198>
- [8] Park J., Jana S.C.: *Macromolecules* **2003**, 36, 8391. <http://dx.doi.org/10.1021/ma0303465>
- [9] Han B., Cheng A., Ji G., Wu S., et al.: *J. Appl. Polym. Sci.* **2004**, 91, 2536. <http://dx.doi.org/10.1002/app.13398>
- [10] Shelley J.S., Mather P.T., De Vries K.L.: *Polymer* **2001**, 42, 5849. [http://dx.doi.org/10.1016/S0032-3861\(00\)00900-9](http://dx.doi.org/10.1016/S0032-3861(00)00900-9)
- [11] Tjong S.C., Bao S.P.: *J. Polym. Sci., Part B* **2004**, 42, 2878. <http://dx.doi.org/10.1002/polb.20161>
- [12] Liu Z., Chen K., Yan D.: *Eur. Polym. J.* **2003**, 39, 2359. [http://dx.doi.org/10.1016/S0014-3057\(03\)00166-6](http://dx.doi.org/10.1016/S0014-3057(03)00166-6)
- [13] Kotek J., Kelnar I., Baldrian J., Šlouf M.: *J. Appl. Polym. Sci.* **2008**, 110, 3752. <http://dx.doi.org/10.1002/app.28859>
- [14] Kelnar I., Kotek J., Kaprálková L., Munteanu B.S.: *J. Appl. Polym. Sci.* **2005**, 96, 288. <http://dx.doi.org/10.1002/app.21374>
- [15] Kelnar I., Rotrekl J., Kotek J., et al.: *Eur. Polym. J.* **2009**, 45, 2760. <http://dx.doi.org/10.1016/j.eurpolymj.2009.06.024>
- [16] Brus J., Urbanova M., Kelnar I., Kotek J.: *Macromolecules* **2006**, 39, 5400. <http://dx.doi.org/10.1021/ma0604946>
- [17] Brus J., Urbanova M.: *J. Phys. Chem. A* **2005**, 109, 5050. <http://dx.doi.org/10.1021/jp0503821>
- [18] Kotek J., Kelnar K., Brus J., Urbanová M.: *e-Polymers* **2009**, 138, 1.
- [19] Brus J., Urbanova M., Strachota A.: *Macromolecules* **2008**, 41, 372. <http://dx.doi.org/10.1021/ma702140g>
- [20] Brus J.: *Solid State Nucl. Magn. Reson.* **2000**, 16, 151. [http://dx.doi.org/10.1016/S0926-2040\(00\)00061-8](http://dx.doi.org/10.1016/S0926-2040(00)00061-8)
- [21] Pramoda K.P., Liu T.: *J. Polym. Sci., Part B* **2004**, 42, 1823. <http://dx.doi.org/10.1002/polb.20061>